AJNR

Tissue segmentation of the brain in Alzheimer disease.

J L Tanabe, D Amend, N Schuff, V DiSclafani, F Ezekiel, D Norman, G Fein and M W Weiner

Tissue Segmentation of the Brain in Alzheimer Disease

Jody L. Tanabe, Diane Amend, Norbert Schuff, Victoria DiSclafani, Frank Ezekiel, David Norman, George Fein, and Michael W. Weiner

PURPOSE: To compare brain tissue in patients with Alzheimer disease with that in elderly control subjects by using high-resolution MR imaging and quantitative tissue-segmentation techniques. **METHODS:** MR imaging of the brain was performed in 21 patients with Alzheimer disease and 17 control subjects. A computerized segmentation program was used to quantify volumes of ventricular and sulcal cerebrospinal fluid (CSF), white matter, cortical gray matter, and white matter signal hyperintensity. Statistical analysis was performed using analysis of variance. **RESULTS:** We found a significant decrease in total brain tissue and cortical gray matter and an increase in the ventricular and sulcal CSF in Alzheimer patients compared with control subjects. There was no difference in the volume of white matter. More white matter signal hyperintensities were found in Alzheimer patients, and a significant interaction between age and group was noted. Neuropsychological test scores correlated significantly with sulcal CSF in patients with Alzheimer disease. **CONCLUSION:** Semiautomated segmentation of MR images of the brains of patients with Alzheimer disease reveals significant brain atrophy attributable to loss of cortical gray matter, which is compatible with the pathologic features of Alzheimer disease. There is also a significant increase in white matter signal hyperintensities. Tissue segmentation may increase our understanding of dementia but, as yet, when used alone, it does not play a role in the premorbid diagnosis of Alzheimer disease.

Index terms: Age and aging; Dementia; Brain, measurements; Magnetic resonance, tissue characterization

Brains of patients with Alzheimer disease are characterized by amyloid plaques and neurofibrillary changes, hippocampal atrophy (1–3), loss of neurons in gray and white matter leading to tissue atrophy and widening of ventricles and sulci (4), and a variable extent of amyloid angiopathy (1). A combination of changes suggesting chronic ischemia, such as myelin and axonal loss and glial proliferation, has been found in white matter (5). Neuroimaging techniques (computed tomography and, more recently, magnetic resonance [MR] imaging) have confirmed the loss of brain tissue, especially gray matter, increased cerebrospinal fluid (CSF), and white matter abnormalities (6–9). Imaging studies have been used to analyze the brain in one of two ways: voluming, which quantitates specific brain regions and anatomic structures with manual tracing, and segmentation, which quantitates the amount of various tissue types (eg, gray matter, white matter, CSF) according to pixel intensity–based features. While numerous neuroimaging investigations have found accelerated whole brain, temporal lobe, and hippocampal atrophy, and significant enlargement of lateral ventricles and cortical sulci in Alzheimer disease (10–12), fewer have addressed differences in volume of tissue (cortical gray matter, white matter, and white matter signal hyperintensities) in Alzheimer disease (13–15). With the use of computer-assisted MR tissue segmentation, some investigators have found reductions in gray matter volume (6, 14, 15) in Alzheimer disease, but these studies have been limited by small sample sizes, inadequate selection of control subjects,

and MR techniques that were not state of the art (thick sections, low in-plane spatial resolution, and low tissue contrast resulting from low signal-to-noise ratio at low field strengths).

Therefore, the major purpose of this study was to confirm, by means of state-of-the-art high-resolution MR images analyzed by semiautomatic segmentation software developed in this laboratory (16), that subjects with Alzheimer disease have greater brain volume loss and sulcal and ventricular enlargement than do elderly control subjects. Brain atrophy may result from loss of either white or gray matter or a combination of the two. Because the dementia of Alzheimer disease is attributed primarily to neuronal loss, cortical gray matter is expected to be reduced to a greater extent than white matter; therefore, the second purpose of this study was to show that the percentage of cortical gray matter loss is greater than that of white matter loss in patients with Alzheimer disease relative to control subjects.

Although white matter is not primarily affected in Alzheimer disease, imaging (6, 7, 9, 17, 18) and pathologic (5, 18) evidence shows that white matter is secondarily affected in Alzheimer disease. Several investigators have described an increase in white matter signal hyperintensities on MR images of patients with Alzheimer disease, while others have been unable to confirm such an increase (19). Therefore, the third purpose of this investigation was to test whether white matter signal hyperintensity is increased in Alzheimer disease. Fourth, we sought a correlation between a global neurocognitive test, the Mini-Mental Status Examination (MMSE), and segmentation variables for subjects with Alzheimer disease. Finally, to determine which segmentation variable provided the best trade-off between specificity and sensitivity in the diagnosis of Alzheimer disease, we conducted a receiver operator characteristic (ROC) analysis.

Materials and Methods

Subjects

Thirty-eight subjects participated in a combined MR imaging/MR spectroscopy protocol. Results from the MR study are reported. Healthy elderly control subjects (n = 17) were recruited by posting fliers in the community. Subjects with Alzheimer disease (n = 21) (12 probable, nine possible) were referred from the UCSF Memory and Alzheimer's Center and the diagnosis was made using criteria established by the National Institutes of Neurological and Communicable Diseases/Alzheimer Disease and Related Disorders Association. A screening interview was conducted to rule out other neurologic or medical disorders that are known to cause dementia and the use of medications with central nervous system effects. A neurologic examination and a neuropsychological test (the MMSE) was administered to both groups.

MR Acquisition

MR studies were performed on a 1.5-T MR system. A sagittal T1-weighted localizer image was obtained, followed by oblique axial double spin-echo images parallel to the planum sphenoidale with the following parameters: 3000/30,80/1 (repetition time/echo time/excitations), 3-mm-thick sections with no section gap, and in-plane resolution of 1×1.4 mm^2. The spin-echo sequence yielded 43 to 46 sections covering the entire brain from the inferior cerebellum to the vertex.

MR Analysis

Semiautomatic, computer interactive thresholding segmentation of the MR images into specific tissue and anatomic compartments was performed. All brains were segmented into areas of ventricular CSF, sulcal CSF, and total brain tissue. All brains but one were then segmented into areas of cortical gray matter, subcortical gray matter, white matter, and abnormal white matter signal hyperintensities. The second level of segmentation was not performed on one brain because of motion artifacts. Images were processed by two trained operators, both blinded to the subjects' identity. Editing of subcortical gray matter regions and white matter signal hyperintensities was performed by one operator. All values were normalized to total number of pixels, expressed as a percentage of intracranial volume.

Preprocessing.—The scalp and skull were first extracted from the image by using a method described by Itti, consisting of four basic steps (thresholding, three-dimensional morphologic erosion, connectivity, and dilatation) (Itti L, *Coregistration for Neuro-imaging Systems [CNS],* Harbor-UCLA Medical Center, Los Angeles, Calif, and Ecole Nationale Superieure des Telecommunications, Paris, France, thesis.) This was followed by estimation and removal of radio frequency field inhomogeneity with a low-pass filter on each image section. Subtraction (the difference between proton density– and T2-weighted) and addition (the sum of the proton density– and T2-weighted) images were created to enhance the ability to see differences between CSF and non-CSF and between gray and white matter, respectively (20).

Image Processing.—On a section-by-section basis, operators applied the threshold technique to classify each pixel as most representative of either CSF or non-CSF samples. Samples were chosen conservatively to represent tissue that definitely belonged to the correct (ie, CSF or non-CSF) classification, leaving a sizable amount of

tissue unclassified. The samples were then used as training sets for a discriminant analysis that used both the proton density– and T2-weighted images to classify each pixel as either CSF or non-CSF. The gray versus white matter discrimination was accomplished in a similar manner. On a section-by-section basis, the operator thresholded the image to classify each non-CSF pixel as most representative of either white matter or gray matter. These samples were chosen conservatively to represent tissue that definitely belonged to the correct (ie, white or gray matter) classification, leaving a sizable amount of tissue unclassified. For each section, the tissue samples were then used as training sets for a discriminant analysis that used both the proton density– and T2-weighted images to classify all non-CSF pixels as either gray or white matter. Ventricular CSF was separated from sulcal CSF, and subcortical nuclei separated from cortical gray matter by manual tracing of the images on a section-by-section basis. Since the automated discriminant analysis will classify areas of abnormal T2 prolongation (white matter signal hyperintensities) as gray matter, these areas also had to be manually separated from normal gray matter. An example of a segmented image and its corresponding proton density–weighted image is shown in Figure 1. All the pixels in each category were then added over the sections and computed as a percentage of total intracranial volume (total pixels). The percentage of white matter was calculated by combining normal white matter with white matter signal hyperintensities. The interoperator reliability was assessed on a nine-brain training set. The interoperator correlations for percentages of ventricular CSF, sulcal CSF, white matter, and gray matter were .99, .99, .91, and .81, respectively. Correlations were not calculated for cortical and subcortical gray matter, since only one operator, a neuroradiologist, performed these measurements.

Statistical Analysis

Two groups (patients with Alzheimer disease and control subjects) and seven dependent variables (ventricular CSF, sulcal CSF, total brain parenchyma, white matter, cortical gray matter, subcortical gray matter, and white matter signal hyperintensities, expressed as a percentage of intracranial volume) were analyzed using the SAS general linear models procedure (SAS Institute, Cary, NC, 1988) with analysis of variance (ANOVA) with multiway interactions, using covariates (ANCOVA) of age and sex.

Correlations between segmentation results and MMSE scores were performed using Pearson correlation tests for each group separately. Cardiovascular risk factors were analyzed with the χ^2 test. ROC curves were generated by using Nonparametric ROC Analysis, Version 2.5 (21). The areas under the curve were compared by using nonparametric methods.

Results

Demographics

Distributions by age, sex, and MMSE score for the groups are shown in Table 1. There was

TABLE 1: Group characteristics of patients with Alzheimer disease and healthy control subjects

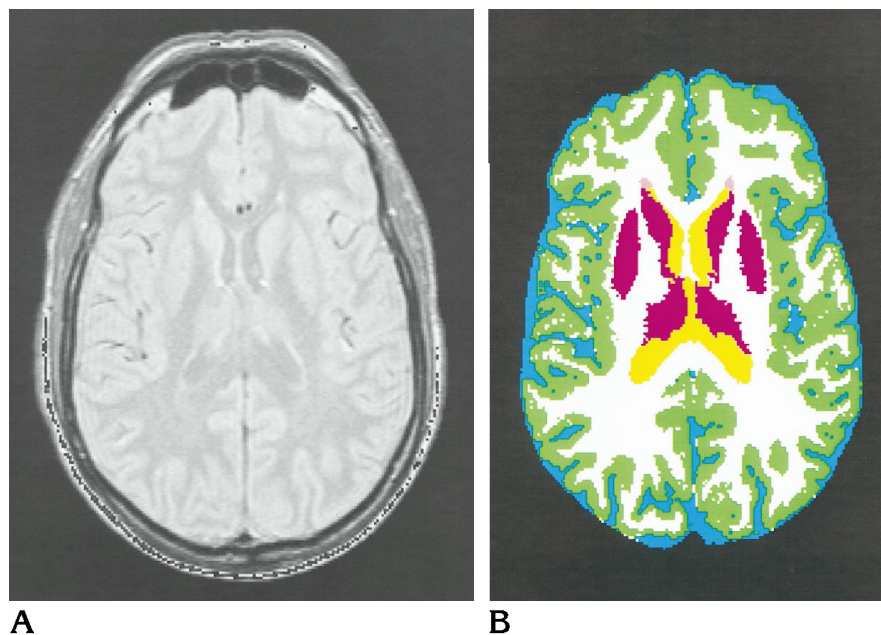|	Alzheimer Patients	Control Subjects
No. of subjects	21	17
Age range	61–78	62–84
Age, mean ± SD	72.0 ± 6.9	70.2 ± 6.2
Men/Women	6/15	8/9
MMSE score, mean ± SD	21 ± 6	29 ± 1

A   B

Fig 1. Proton density–weighted (*A*) and corresponding segmented (*B*) MR images. *Green* indicates cortical gray matter; *white*, white matter; *yellow*, ventricular CSF; *blue*, sulcal CSF; *purple*, subcortical gray matter; and *pink*, periventricular white matter signal hyperintensity.

TABLE 2: Segmentation results expressed as a percentage of intracranial volume for patients with Alzheimer disease and healthy control subjects

Tissue Type	Alzheimer Patients	Control Subjects	P*	Percentage of Difference
Brain	73.6 ± .8	78.5 ± .9	.0003	−6
Ventricular CSF	4.8 ± .2	2.7 ± .3	.0001	+78
Sulcal CSF	21.9 ± .7	18.8 ± .8	.0054	+17
Cortical gray matter	34.7 ± .5	38.5 ± .5	.0001	−10
Subcortical gray matter	2.0 ± .2	2.2 ± .1	NS	...
White matter, normal plus WMSH	36.9 ± .7	37.8 ± .7	NS	...
WMSH	1.7 ± .2	.9 ± .2	.005†	+88

Note.—Values are least-squared mean ± SD. WMSH indicates white matter signal hyperintensities; NS, not significant.
* P value calculated from multiway ANOVA.
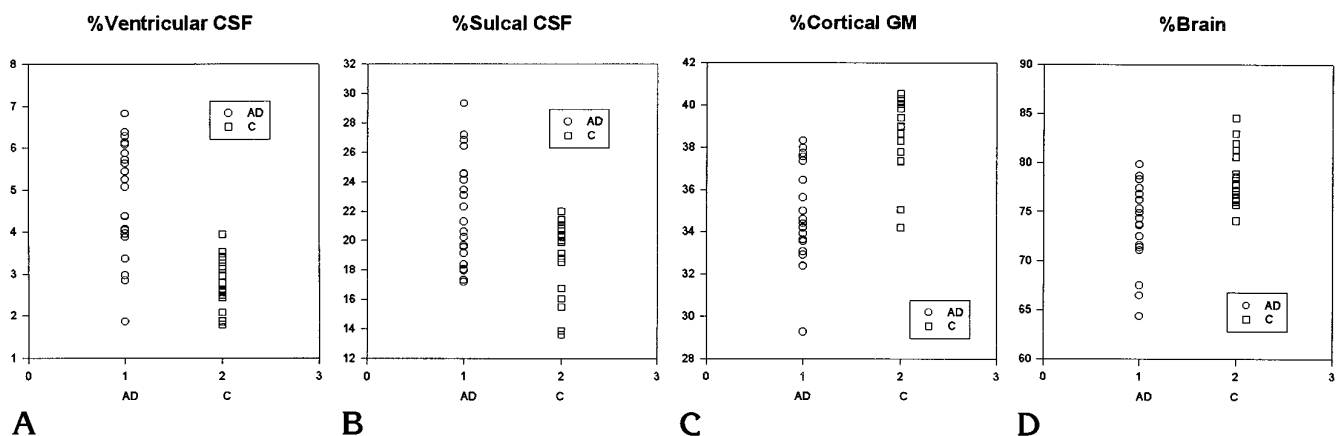† Significant interaction between group and age.

Fig 2. Scatterplots of percentage of ventricular CSF (*A*), sulcal CSF (*B*), cortical gray matter (*GM*) (*C*), and total brain parenchyma (*D*) as a percentage of intracranial volume in patients with Alzheimer disease (*AD*) and healthy control subjects (*C*).

no difference in mean age between Alzheimer patients and control subjects.

Segmentation

Significant differences were found between Alzheimer patients and control subjects in the percentage of total brain tissue, ventricular CSF, sulcal CSF, and cortical gray matter. Neither sex nor age contributed significantly to group differences for these variables. The percentage of white matter signal hyperintensities was significantly greater in Alzheimer patients than in control subjects, and there was also an interaction between group and age.

Table 2 shows that there was a large (78%) mean difference in percentage of ventricular volume between the groups (4.8% in Alzheimer patients versus 2.7% in control subjects) followed by the percentage of sulcal CSF, which was larger in Alzheimer patients by 17% than in control subjects (22% versus 19%). Total brain and cortical gray matter were significantly smaller in Alzheimer patients by 6% and 10%, respectively (total brain, 74% versus 79%; cortical gray matter, 35% versus 39% in Alzheimer patients versus control subjects, respectively). Figure 2 shows an overlap between Alzheimer patients and control subjects for all significant variables. There was no significant difference in subcortical nuclei or total white matter, the latter defined as the sum of normal-appearing white matter plus white matter signal hyperintensities.

Figure 3 shows the effect of age on white matter signal hyperintensities in Alzheimer patients and control subjects. The percentage of these areas of hyperintensity, like the other measures, is expressed as a percentage of total intracranial volume. Each point on the scatterplot represents a subject and shows that the overall value for percentage of hyperintensity is larger in Alzheimer patients ($P < .005$), and that there is a significant interaction ($P < .02$) be-
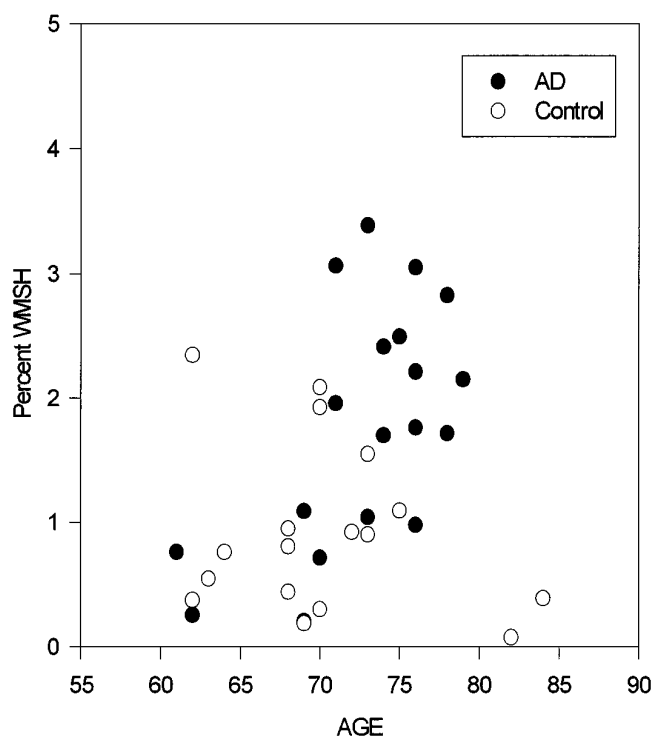
Fig 3. Percentage of white matter signal hyperintensities (*WMSH*) as a function of age in patients with Alzheimer disease (*AD*) and healthy control subjects (*Control*).

Fig 4. Receiver operator characteristic curves for segmentation variables.

tween age and group, such that the accumulation of hyperintensities is accelerated in older subjects with Alzheimer disease.

Figure 4 plots the ROC curves for the four significant segmentation variables (percentage of cortical gray matter, brain, ventriclar CSF, and sulcal CSF). Table 3 shows areas under the curve in descending order for cortical gray matter, brain, ventriclar CSF, and sulcal CSF (.90, .89, .84, 72, respectively). The area under the curve was higher and significantly different for cortical gray matter than for sulcal CSF ($P <$ .05).

Correlations Between Segmentation, Clinical Indexes, and MMSE Scores

In the Alzheimer group, a significant correlation between MMSE score and percentage of sulcal CSF was found ($r = -.5525$, $P <$ .03). In the control group, no significant correlation was found between the MMSE score and segmentation variables. There was no significant difference in cardiovascular risk factors between the groups (Table 4).
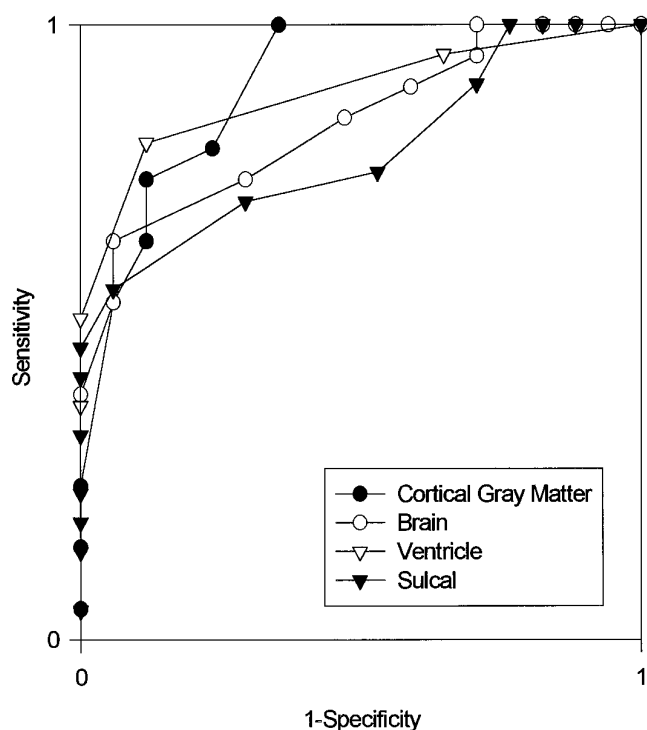
TABLE 3: Areas under the curve for ROC analysis

Tissue Type	Areas under the Curve
Cortical gray matter	.90 ± .05*
Brain	.84 ± .06
Ventricular CSF	.89 ± .05
Sulcal CSF	.72 ± .08

* $P <$ .05 compared with sulcal CSF (one-tailed t test).

Discussion

Neuroimaging studies in patients with Alzheimer disease can be quantitated by one of two methods: segmentation into different tissue types using pixel intensity–based features and anatomic voluming using manual tracing of brain structures. This article reports the results of tissue segmentation of high-resolution MR images in patients with Alzheimer disease. The major findings are that in Alzheimer patients there is significantly greater total brain atrophy and significantly greater enlargement of ventricular and sulcal CSF volumes; cortical gray matter is reduced significantly whereas the volume of white matter is unchanged; abnormal white matter signal hyperintensities are greater; there is a slight but significant correlation between

TABLE 4: Cardiovascular risk factors for Alzheimer patients and control group

	Alzheimer Patients (n = 21)	%	Control Group (n = 17)	%
Hypertension	4	19	3	18
Diabetes mellitus	1	5	0	0
Smoking (>10 pack-year)	4	19	6	35

Note.—χ^2 = 1.54, degrees of freedom = 2, $P > .25$.

cognitive performance and percentage of sulcal CSF; and, among the segmentation measures, cortical gray matter provided the best trade-off between specificity and sensitivity.

We found significantly greater brain loss and ventricular and sulcal enlargement in subjects with Alzheimer disease compared with age-matched healthy control subjects. Our results confirm previous studies that used both linear (8) and volumetric (6, 13, 15, 22) MR techniques to assess brain loss in Alzheimer disease. Previous studies have been limited by small sample sizes and only partial brain segmentation (15), inadequate selection of control subjects, and MR techniques that were not state of the art; that is, images were acquired with a section gap (6, 13, 15) thereby excluding up to 30% of the brain; the sections were relatively thick (6 to 10 mm) (14, 22) and were obtained on systems with lower signal-to-noise ratio caused by low field strength (22, 23). These technical differences need to be considered and may explain, for example, the conflicting results reported by Desmond et al (23), who found no difference in mean brain volume between Alzheimer patients and control subjects. Possible explanations for this discrepancy are reduced signal-to-noise ratio resulting from a low-field system and subjectivity introduced by use of a manual tracing technique.

It is well established pathologically and within vivo imaging that, in normal aging, the total brain volume decreases while ventricular and sulcal CSF volumes increase in a linear or curvilinear fashion (24–27), thus emphasizing the need for using age-matched control subjects. The difference in the percentage of ventricular volume in patients with Alzheimer disease compared with control subjects was 78% in our study, which was much larger than the difference in percentage of sulcal CSF volume, which was about 17% greater in Alzheimer patients. Other investigators have also found more pronounced ventricular than sulcal enlargement (8, 15, 22, 28), and longitudinal studies have shown that subjects with Alzheimer disease

have an accelerated rate of ventricular enlargement compared with control subjects, suggesting that ventricular size is a sensitive, albeit less specific, marker for Alzheimer disease (29). This raises the question of whether ventricular enlargement simply reflects generalized brain atrophy.

Our data suggest that cortical gray matter atrophy could account for much, if not all, of the ventriculomegaly, as there is little to no decrease in the total white matter in Alzheimer disease. The second finding of this study was a significant reduction in the volume of cortical gray matter and no significant decrease in white matter volume in Alzheimer patients compared with elderly control subjects. Since Alzheimer disease is characterized by cortical neuronal loss, it is expected that the percentage of cortical gray matter would be diminished to a greater extent than that of white matter. Our results agree with others: Rusinek et al (14) found significant gray matter reduction in Alzheimer disease using inversion recovery sequences (which are very time consuming) and Jernigan et al (6) reported significant loss of gray but not white matter in Alzheimer subjects. However, Jernigan et al used control subjects whose mean age was 16 years younger than the Alzheimer group, and gray matter volume is known to decrease with normal aging. Thus, we were able to show accelerated cortical gray but not white matter atrophy in Alzheimer disease using standard spin-echo sequences and age-matched control subjects. Total gray matter (sum of cortical and subcortical) remained significantly different, but subcortical gray matter alone was the same between groups.

The significance and specificity of cortical gray matter atrophy remains uncertain. For example, can we distinguish dementias primarily affecting gray matter (Alzheimer disease, Tay-Sachs disease) from those primarily affecting white matter (ischemic vascular dementia or adult adrenoleukodystrophy) by means of tissue segmentation? In this study, we defined white matter as the sum of normal white matter

plus white matter signal hyperintensities. We recognize the potential inaccuracy of designating the entire volume of these areas as white matter. Our rationale for this definition is that in Alzheimer disease an area of T2 prolongation is associated with varying degrees of ependymal denudation, gliosis, and loss of myelinated axons (5). It would be difficult to quantitate these pathologic entities separately and impossible to separate them with the use of intensity-based segmentation.

The third finding was that the volume of white matter signal hyperintensity was significantly larger in Alzheimer patients than in control subjects. Most investigators have reported semi-quantitative increases in hyperintensity in Alzheimer disease (7, 8, 17, 30, 31), while only a few others found no difference (19). Two groups (6, 15) quantitatively analyzed hyperintensity in a manner similar to ours with conflicting results. Mackay et al (15) found no difference in amount of hyperintensity in Alzheimer and control subjects, but their study had a small sample size and used thick sections and an intersection gap. Jernigan et al (6), on the other hand, reported a significant difference, but their control subjects were substantially younger (16 years) than their Alzheimer patients. It is well known that white matter changes, seen on MR images as areas of white matter signal hyperintensities, are frequently found in healthy elderly persons (32). Disparate results could reflect differences in cardiovascular status, which were not controlled for in the previous studies. The exclusion of all subjects with any cardiovascular risk factors may explain the findings in the study by Leys et al (19), who reported no significant difference in white matter signal hyperintensity. In our study, no Alzheimer subject had had a cortical stroke and, although we did not specifically control for vascular risk factors, a brief screening revealed no significant difference in hypertension, smoking, or diabetes mellitus compared with control subjects (Table 4). Persons suspected of having vascular dementia were excluded from the study. In addition to differences in the amount of white matter signal hyperintensities, an interaction between Alzheimer disease and age was found (Table 2). The scatterplot in Figure 3 suggests that older subjects with Alzheimer disease have more signal hyperintensities than older control subjects, while younger subjects with Alzheimer disease may not. We interpret these results as suggesting

that older subjects with Alzheimer disease are more susceptible to white matter disease. Future investigations that prospectively control for vascular risk factors and age may clarify the prevalence of white matter disease in Alzheimer patients.

There is some evidence that suggests a higher prevalence of white matter signal hyperintensities among patients with Alzheimer disease (5, 18). Some authors have raised the possibility of a distinct white matter disorder in Alzheimer disease with a pathogenesis the same as that causing cortical damage (7, 18). Conversely, an extensive pathologic study by Brun and Englund (5) concluded that white matter disease (characterized by partial loss of myelin, axons, and oligodendroglia) occurred independent of the gray matter degeneration in Alzheimer disease, was probably not the result of cortical wallerian degeneration, and was perhaps the result of chronic hypoperfusion.

If the pathogenesis of white matter disease is independent of the gray matter degeneration in Alzheimer disease, what is the clinical significance of white matter signal hyperintensities? It appears to have no significant cognitive sequelae, either in healthy elderly persons (32) or in Alzheimer patients. Like others, we found no correlation between white matter signal hyperintensities and MMSE score (19, 31, 33–35). This is not surprising, since the structures critical to cognitive function in Alzheimer disease are thought to be the hippocampus and temporoparietal cortex. The significance of signal hyperintensity in Alzheimer disease remains uncertain; rather than correlating it to cognitive level, future investigations should focus on correlations with tests of subcortical function; for example, executive control function (36) or gait and urinary function (34).

Our fourth finding was a mild but significant correlation between MMSE score and percentage of sulcal CSF ($r = -.552$, $P < .02$). No other segmentation measure correlated significantly with MMSE score. Perhaps sulcal CSF, more than the other measures, closely reflects neuronal loss resulting in cognitive impairment. Although significant correlations between MMSE score and brain atrophy (13, 22), hippocampal volumes (37), and gray matter (13) have been reported in Alzheimer disease, such correlations have generally been weak.

The fifth objective of this study was to determine which tissue segmentation variable of-

fered the best performance in the diagnosis of Alzheimer disease using ROC analysis. ROC curves provide a visual assessment of the trade-off between sensitivity and specificity for different diagnostic tests and enable quantification and comparison of test performance by calculating the area under the ROC curve (21). Figure 4 shows the ROC curves for four variables: cortical gray matter, ventricular CSF, sulcal CSF, and brain. Table 3 shows that the area under the curve was highest for cortical gray matter (.90 ± .05), which was significantly larger than the area under the curve for percentage of sulcal CSF (.72 ± .08). It is possible that the high performance of cortical gray matter by ROC analysis reflects the fact that cortical neurons are directly involved in Alzheimer disease.

A potential source of bias in this study could be the difference in the distribution of age and sex between the groups. Despite a gender imbalance (six men and 15 women in the Alzheimer group, eight men and nine women in the control group), covariate analysis showed no group effect attributable to gender. The specific breakdown of ages between subjects in the two groups can be inferred from the scatterplot in Figure 3, which confirms no significant age bias. Other possible sources of error include a technical limitation inherent to all segmentation processing, that of partial volume averaging. Each pixel of the brain is assigned to a particular tissue type, even though, in reality, the pixel is composed of several tissue types. By limiting our section thickness, eliminating intersection gaps, and using high in-plane resolution, we attempted to minimize partial volume effects. Third, since our objective was to assess total white matter volume in Alzheimer disease, we defined white matter as "normal white matter" plus white matter signal hyperintensities. It would have been impossible to separate normal white matter fibers within an area of hyperintensity. Fourth, gray–white matter contrast is typically superior on heavily T1-weighted images compared with T2-weighted images. However, at the time this study was undertaken, the segmentation program was limited to processing only T2-weighted images. Since then, we have developed the software to process both T1- and T2-weighted images and found no significant differences in the gray and white matter calculations between the two methods.

In summary, high-resolution quantitative MR tissue segmentation of the brain in Alzheimer disease reveals significant increases in whole brain loss, ventricular CSF volume, and sulcal CSF volume. Consistent with pathologic observations, this atrophy can be attributed to a reduction in cortical gray matter, as the volume of white matter is unchanged in Alzheimer disease. Subjects with Alzheimer disease have more abnormal white matter signal hyperintensities than do age-matched control subjects with similar cardiovascular risk factors. In addition, the accumulation of signal hyperintensities appears to accelerate in older patients with Alzheimer disease compared with older control subjects. Significant overlap between groups limits the use of MR tissue segmentation as a premorbid diagnostic tool, but it may improve our understanding of Alzheimer disease.

Acknowledgments

References

1. Wisniewski HM, Wegiel J. Neuropathology of Alzheimer's disease. *Neuroimaging Clin N Am* 1995;5:45–57
2. Rewcastle NB. Neurodegenerative disease. In: Davis RL, Robertson DM, eds. *Textbook of Neuropathology*. Baltimore, Md: Williams & Wilkins; 1991:908–919
3. Braak H, Braak E. Neuropathological staging of Alzheimer-related changes. *Acta Neuropathol* 1991;82:239–259
4. Gado M, Hughes CP, Danziger W, et al. Aging, dementia, and brain atrophy: a longitudinal computed tomographic study. *AJNR Am J Neuroradiol* 1983;4:699–702
5. Brun A, Englund EA. White matter disorder in dementia of the Alzheimer type: a pathoanatomical study. *Ann Neurol* 1986;19:253–262
6. Jernigan TL, Salmon DP, Butters N, Hesselink JR. Cerebral structure on MRI, part II: specific changes in Alzheimer's and Huntington's diseases. *Biol Psychiatry* 1991;29:68–81
7. Fazekas F, Chawluk JB, Alavi A, Hurtig HI, Zimmerman RA. MR signal abnormalities at 1. 5T in Alzheimer's dementia and normal aging. *AJNR Am J Neuroradiol* 1986;8:421–426
8. Schmidt R. Comparison of magnetic resonance imaging in Alzheimer's disease, vascular dementia and normal aging. *Eur Neurol* 1992;32:164–169
9. Kawamura J, Meyer JS, Ichijo M, Kobari M, Terayama Y, Weathers S. Leuko-araiosis and cerebral hypoperfusion compared in elderly normals and Alzheimer's dementia. *J Neurol Neurosurg Psychiatry* 1993;56:182–187
10. Sullivan EV, Shear PK, Mathalon DH, et al. Greater abnormalities of brain cerebrospinal fluid volumes in younger than in older patients with Alzheimer's disease. *Arch Neurol* 1993;50:359–373
11. deLeon MJ, George AE, Stylopoulos AL, et al. Early marker for Alzheimer's disease: the atrophic hippocampus. *Lancet* 1989;1:672–673
12. Jobst KA, Smith AD, Szatmari M, et al. Detection in life of confirmed Alzheimer's disease using a simple measurement of medial

temporal lobe atrophy by computed tomography. *Lancet* 1992; 340:1179–1183

13. Tanna NK, Kohn MI, Horwich DN, et al. Analysis of brain and cerebrospinal fluid volumes with MR imaging: impact on PET data correction for atrophy. *Radiology* 1991;178:123–130

14. Rusinek H, de Leon MJ, George AE, et al. Alzheimer disease: measuring loss of cerebral gray matter with MRI imaging. *Radiology* 1991;178:109–114

15. Mackay S, Ezekiel F, DiSclafani V, et al. Alzheimer's disease and subcortical ischemic vascular dementia: evaluation by combining MRI segmentation and H-1MR spectroscopic imaging. *Radiology* 1996;198:537–545

16. DiSclafani V, Ezekiel F, Meyerhoff D, et al. Brain atrophy and cognitive function in older abstinent alcoholic men. *Alcohol Clin Exp Res* (in press)

17. Coffman JA, Torello MW, Bornstein RA, Chakeres D, Burns E, Nasrallah HA. Leukoaraiosis in asymptomatic adult offspring of individuals with Alzheimer's disease. *Biol Psychiatry* 1990;27: 1244–1248

18. Scheltens PH, Barkhof F, Valk J, et al. White matter lesions on magnetic resonance imaging in clinically diagnosed Alzheimer's disease. *Brain* 1992;115:735–748

19. Leys D, Soetaert G, Petit H, Fauquette A, Pruvo JP, Steinling M. Periventricular and white matter MRI hyperintensities do not differ between Alzheimer's disease and normal aging. *Arch Neurol* 1990;47:524–527

20. Lim KO, Pfefferbaum A. Segmentation of MR brain images into cerebrospinal fluid spaces, white and gray matter. *J Comput Assist Tomogr* 1989;13:588–593

21. Vida SA. Computer program for non-parametric receiver operating characteristic analysis. *Comput Methods Programs Biomed* 1993;40:95–101

22. Murphy DG, DeCarli CD, Gillette JA, et al. Volumetric magnetic resonance imaging in men with dementia of the Alzheimer type: correlations with disease severity. *Biol Psychiatry* 1993;34:612–621

23. Desmond PM, O'Brien JT, Tress BM, et al. Volumetric and visual assessment of the mesial temporal structures in Alzheimer's disease. *Aust N Z J Med* 1994;24:547–553

24. Jernigan TL, Press GA, Hesselink JR. Methods for measuring brain morphologic features on magnetic resonance images: validation and normal aging. *Arch Neurol* 1990;47:27–32

25. Blatter DD, Bigler ED, Gale SD, et al. Quantitative volumetric analysis of brain MR: normative database spanning 5 decades of life. *AJNR Am J Neuroradiol* 1995;16:241–251

26. Murphy DG, DeCarli C, Schapiro MB, Rapoport SI, Horwitz B. Age-related differences in volumes of subcortical nuclei, brain matter, and cerebrospinal fluid in healthy men as measured with magnetic resonance imaging. *Arch Neurol* 1992;49:839–845

27. Pfefferbaum A, Mathalon DH, Sullivan EV, Rawles JM, Zipursky RB, Lim KO. A quantitative magnetic resonance imaging study of changes in brain morphology from infancy to late adulthood. *Arch Neurol* 1994;51:874–887

28. Seab JP, Jagust WJ, Wong STS, Roos MS, Reed BR, Budinger TF. Quantitative NMR measurements of hippocampal atrophy in Alzheimer's disease. *Magn Reson Med* 1988;8:200–208

29. Luxenberg JS, Haxby JV, Creasey H, Sundaram M, Rapoport SI. Rate of ventricular enlargement in dementia of the Alzheimer type correlates with rate of neuropsychological deterioration. *Neurology* 1987;37:1135–1140

30. McDonald WM, Krishnan KR, Doraiswamy PM, et al. Magnetic resonance findings in patients with early-onset Alzheimer's disease. *Biol Psychiatry* 1991;29:699–710

31. Waldemar G, Christiansen P, Larsson HB, et al. White matter magnetic resonance hyperintensities in dementia of the Alzheimer type: morphological and regional cerebral blood flow correlates. *J Neurol Neurosurg Psychiatry* 1994;57:1458–1465

32. Brant-Zawadzki M, Fein G, Van Dyke C, Kiernan R, Davenport L, deGroot JMR. Imaging of the aging brain: patchy white matter lesions and dementia. *AJNR Am J Neuroradiol* 1985;6:675–682

33. Wahlund LO, Basun H, Almkvist O, Andersson-Lundman G, Julin P, Saaf J. White matter hyperintensities in dementia: does it matter? *Magn Reson Imaging* 1994;3:387–394

34. Bennett DA, Gilley DS, Wilson RS, Huckman MS, Fox JH. Clinical correlates of high signal lesions on magnetic resonance imaging in Alzheimer's disease. *J Neurol* 1992;239:186–190

35. Marder K, Richards M, Bello J, et al. Clinical correlates of Alzheimer's disease with and without silent radiographic abnormalities. *Arch Neurol* 1995;52:146–151

36. Breteler MMB, van Swieten JC, Bots ML, et al. Cerebral white matter lesions, vascular risk factors, and cognitive function in a population-based study: the Rotterdam study. *Neurology* 1994; 44:1246–1252

37. Lehericy S, Baulac M, Chiras J, et al. Amygdalohippocampal MR volume measurements in the early stages of Alzheimer disease. *AJNR Am J Neuroradiol* 1994;15:927–937